

In Utero Ultrafine Particulate Exposure Yields Sex- and Dose-Specific Responses to Neonatal Respiratory Syncytial Virus Infection

Carmen Lau, Jonathan C. Behlen, Alexandra Myers, Yixin Li, Jiayun Zhao, Navada Harvey, Gus Wright, Aline Rodrigues Hoffmann, Renyi Zhang, and Natalie M. Johnson*



Cite This: *Environ. Sci. Technol.* 2022, 56, 11527–11535



Read Online

ACCESS |

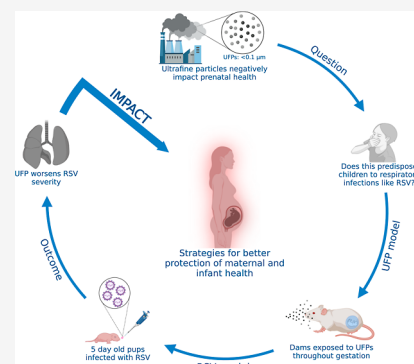
Metrics & More

Article Recommendations

Supporting Information

ABSTRACT: Exposure to particulate matter (PM) is associated with lower respiratory tract infections. The role of ultrafine particles (UFPs, $\leq 0.1 \mu\text{m}$) in respiratory disease is not fully elucidated, especially in models of immunologically immature populations. To characterize the effects of maternal UFP exposure on neonatal infection, we exposed time-mated C57Bl/6n mice to filtered air or UFPs at a low dose (LD, $\sim 55 \mu\text{g}/\text{m}^3$) and high dose (HD, $\sim 275 \mu\text{g}/\text{m}^3$) throughout gestation. At 5 days of age, offspring were infected with a respiratory syncytial virus (RSV) strain known to mimic infant infection or sham control. Offspring body weights were significantly reduced in response to infection in the LD RSV group, particularly females. Pulmonary gene expression analysis demonstrated significantly increased levels of oxidative stress- and inflammation-related genes in HD-exposed male offspring in sham and RSV-infected groups. In males, the highest grade of inflammation was observed in the HD RSV group, whereas in females, the LD RSV group showed the most marked inflammation. Overall, findings highlight neonatal responses are dependent on offspring sex and maternal UFP dose. Importantly, infant RSV pathology may be enhanced following even low dose UFP exposure signifying the importance of preventing maternal exposure.

KEYWORDS: ultrafine particulate matter, prenatal exposure, lower respiratory tract infection, respiratory syncytial virus, neonatal mouse model



1. INTRODUCTION

Maternal exposure to particulate matter (PM) air pollution is a major cause of infant morbidity and mortality largely due to complications related to preterm birth, infant low birth weight, and lower respiratory tract infections (LTRIs) in children.^{1–5} Studies on early life exposure to fine PM ($\text{PM}_{2.5}$) demonstrate impacts on fetal lung development and pulmonary health in a variety of ways that may persist throughout childhood.⁶ Epidemiological studies show children are at increased risk for severe respiratory infections following early childhood or prenatal $\text{PM}_{2.5}$ exposure.^{7,8} Darrow et al. observed significant associations between the organic carbon fraction of $\text{PM}_{2.5}$ and hospitalizations for pneumonia and upper respiratory infections and suggestive associations with bronchiolitis/bronchitis among children 1–4 years of age. Associations were also observed for the sulfate fraction, a secondary pollutant formed primarily from coal-fired power plant emissions. Jedrychowski et al. revealed an increased risk of recurrent broncho-pulmonary infections in children correlated with maternal $\text{PM}_{2.5}$ exposure in a dose–response manner, highlighting the 24 h mean level $20 \mu\text{g}/\text{m}^3$ may better protect infants in comparison to the current U.S. EPA standard $35 \mu\text{g}/\text{m}^3$. Currently, there are no specific regulatory standards set for the ultrafine particle (UFP) fraction, particles with a diameter less than 100 nm, despite recent evidence that UFPs can

influence risk of hospitalization for respiratory infection in children.⁹ The precise mechanisms in how prenatal exposure enhances infant respiratory infection remains largely uncharacterized in response to viral infections and in respect to the role of offspring sex.

Previous experimental models probing mechanisms of skewed immune responses have combined neonatal PM (mean diameter $0.2 \mu\text{m}$) with influenza infection. Lee et al. showed neonatal exposure to radical containing-PM significantly enhanced pulmonary oxidative stress and influenza infection severity via increased presence of regulatory T cells (Tregs).¹⁰ In follow up work, increases in the immunosuppressive cytokine IL-10 and pulmonary Tregs were confirmed to suppress adaptive T cell responses underlying enhanced infection severity.¹¹ Analogous to these findings, our laboratory developed an exposure model wherein pregnant C57Bl/6 or Balb/c mice were exposed to UFPs with a peak diameter $\sim 50 \text{nm}$.¹² In this model, C57Bl/6 offspring prenatally exposed to

Received: April 20, 2022

Revised: July 12, 2022

Accepted: July 14, 2022

Published: August 4, 2022



UFPs and challenged with an allergen from 1 to 4 weeks of age demonstrated an immunosuppressive phenotype evidenced by loss of IL-13 and IL-17 pulmonary cytokine expression and increased IL-10 levels in serum. Building off this model, the objective of the current study was to evaluate the impact of prenatal UFP exposure on response to neonatal respiratory syncytial virus (RSV) infection, an important cause of infant bronchiolitis and related hospitalizations.

RSV is an enveloped, single stranded, negative sense RNA virus in the genus *Pneumovirus* that has a high morbidity and significant mortality among pediatric patients characterized by bronchiolitis and respiratory failure.^{13–15} RSV infection is the leading cause of infant hospitalization, and it has been estimated that 2.1 million children in the U.S. alone require medical attention for RSV infection every year.¹⁶ Children are much more susceptible due to their diminutive bronchi and bronchiolar diameter that easily become obstructed with mucus, inflammatory cells, and sloughed epithelium.¹⁴ Moreover, infant RSV infection presents with increased Th2 cytokine production and decreased Th1 response, which has been modeled in neonatal mice successfully with a chimeric strain (rA2-19F) to replicate key features of infant viral infection.^{13–15} We hypothesized maternal UFP exposure may alter offspring pulmonary immune responses to enhance RSV disease severity. To test our hypothesis, we exposed time-mated C57Bl/6n mice to filtered air (FA) or UFPs at a low dose (LD, $\sim 55 \mu\text{g}/\text{m}^3$) and high dose (HD, $\sim 275 \mu\text{g}/\text{m}^3$) and challenged their offspring with RSV or sham (control) shortly after birth to evaluate infection responses.

2. MATERIALS AND METHODS

2.1. UFP Generation and Mouse Exposure Model. PM generation followed methods developed by Rychlik et al.¹² 2019, with adaptations to accommodate individual housing within whole body exposure chambers and two doses detailed by Behlen et al.¹⁹ 2021. Briefly, air was continuously pumped into three separate chambers where individually housed pregnant dams were separated into FA, LD, or HD exposure groups. Each chamber had a HEPA FA pump where the LD and HD chambers had an additional PM solution pump. We employed a multicomponent aerosol mixture consisting of ammonium nitrate, ammonium sulfate, diesel exhaust PM (NIST, SRM 2975), and potassium chloride, with the mass fractions of 44, 39, 10, and 7%, respectively. Real-time mass concentration analysis was performed using a tandem differential mobility analyzer and condensation particle counter to ensure consistent particle concentrations within chambers throughout the exposure duration.

Mice were housed in a climate-controlled room with 12/12 h light/dark cycle at an AAALAC approved facility at Texas A&M University. Mice had access to standard chow, 19% protein extruded rodent diet (Teklad Global Diets), and water *ad libitum* except during exposure periods. Male and female C57Bl/6n 8 to 10 week-old mice (Jackson Laboratory, Bar Harbor, ME) were time-mated. The presence of a vaginal plug defined gestational day (GD) 0.5. Beginning on GD0.5, dams were randomized and placed into exposure chambers where they were exposed to either FA ($n = 14$), LD ($n = 12$), or HD ($n = 13$) from 0800 to 1400 h (6 h) daily through GD17.5. Following exposure, mice were removed to individual housing and allowed to deliver spontaneously (Figure S1).

2.2. Offspring RSV Challenge. Litters from all three maternal exposure groups were randomly allocated to postnatal

groups, including experimental (RSV-infected) or control (sham-infected). A chimeric RSV strain, rA2-19F, previously shown to elicit an aberrant immune response in neonatal mice mimicking human infant infection, was provided by Dr. Martin Moore (University of Emory, Atlanta, GA). This strain was passaged in our laboratory in HEp-2 cells (ATCC, Manassas, VA) in serum-free-media (SFM4MegaVir, Hyclone, Logan, UT). The day of birth was defined as postnatal day (PND) 1. On PND5, offspring were briefly anesthetized with 4.5% isoflurane in oxygen and infected intranasally with either 10 μL RSV (10^6 virus particles/mL) in culture media or 10 μL culture media alone (5 μL in each nostril). Body weights were recorded daily. Male and female offspring within each litter were randomly assigned to necropsy groups to evaluate viral load 3 days post-infection (dpi) ($n = 61$) and pulmonary immune responses 9 dpi, including collection of bronchoalveolar lavage fluid (BALF) ($n = 71$), lung inflation for fixation and subsequent histological analysis ($s = 65$), and T cell profiling via flow cytometry ($n = 21$). Additional collection details provided in Supplemental Methods.

2.3. Gene Expression Analysis. Total RNA was extracted from offspring lungs collected 9 dpi using TRIzol reagent according to manufacturer's protocol. RNA was quantified with a Nanodrop Spectrophotometer with ≥ 1.8 260/280 nm absorbance values. Following purification, cDNA was reverse transcribed (Qiagen QuantiTect Reverse Transcription), and transcription levels of key genes related to oxidative stress and immune responses (*Nrf2*, *Nqo1*, *NF- κ B*) were analyzed using SYBR Green qRT-PCR (Applied Biosystems Power SYBR Green PCR Master Mix) on a Roche LightCycler 96 System. Relative expression was calculated using $2^{-\Delta\Delta C_T}$ with *Gapdh* as the reference gene.

2.4. Pulmonary Immune Responses. BALF cellularity was assessed 9 dpi. Briefly, BALF was collected by tracheal cannulation and washing the lungs with 0.25 mL of sterile PBS. Total leukocyte counts and differentials were determined by a clinical pathologist blinded to a treatment group. Remaining lungs from this necropsy group were frozen in liquid nitrogen and stored at -80 °C for qRT-PCR. Likewise, 9 dpi in a separate subset of offspring, lungs were excised, inflated at a constant pressure of 25 cm, and fixed with zinc formalin. Additionally, nasal tissues were collected and decalcified in Davidson's solution for 3 days. Lung and nasal tissue were placed in 70% EtOH and processed and stained with hematoxylin and eosin (H&E) to identify cellular infiltrates and periodic acid–Schiff (PAS) for goblet cell analysis. All histological assessments were carried out by an anatomic pathologist blinded to treatment groups. A scoring system was used as follows to rate inflammation severity: 0 (none to minimal), 1 (mild), 2 (moderate), and 3 (marked). The number of goblet cells were assessed in 20 different 10 \times fields using a scoring system corresponding to the percentage of goblet cells in the bronchiolar epithelial cells, as previously described.¹⁷ Last, lungs from a separate subset of offspring sacrificed 9 dpi were perfused with sterile PBS to deplete red blood cells prior to processing into single cell suspensions for flow cytometry (details in Supplemental Methods). Cells were stained with antibodies for CD3, CD4, CD8, IFN γ , and IL-4 to determine CD8+ and CD4+ Th1/Th2 responses, respectively. Additionally, to evaluate T regulatory cells (Tregs), cells were stained with antibodies for CD25 and FOXP3. Stained samples were analyzed using a Beckman Coulter Moflo Astrios high

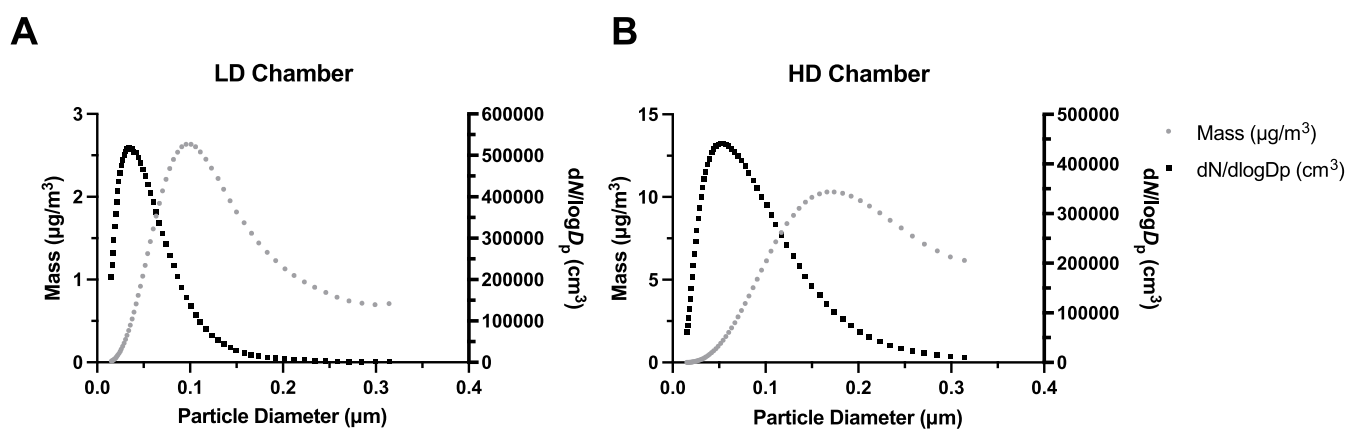


Figure 1. Ultrafine particle characterization showing the size and concentration distributions. (A) LD PM particle size (black) and concentration (gray) distribution, with a peak particle diameter of $0.034 \mu\text{m}$ (34 nm). (B) HD PM particle size (black) and concentration (gray) distribution, with a peak particle diameter of $0.052 \mu\text{m}$ (52 nm).

speed cell sorter. Data was analyzed using FlowJo Software. Gating strategies are depicted in Figures S7–S10.

2.5. Pulmonary Viral Load. To determine the number of infectious virus particles in RSV-challenged offspring, pup lungs were quickly excised 3 dpi, frozen in liquid nitrogen, and stored at $-80 \text{ }^\circ\text{C}$ until median tissue culture infectious dose (TCID_{50}) analysis. For this assay, Vero cells (ATCC, Manassas, VA) were grown to confluency in 96 well plates. Media was removed, and $90 \mu\text{L}$ infection media was added to the wells. Offspring lung tissue was homogenized in 1 mL cold cell culture media, filtered with a $40 \mu\text{m}$ cell filter, and the homogenate was added to the wells in duplicate. Samples were serially diluted, and plates were incubated at $37 \text{ }^\circ\text{C}$ with 5% CO_2 for 7 days. Wells were checked at days 4 and 7 for cytopathic effect (CPE), and TCID_{50} (virions/mL) was calculated as previously described.¹⁸

2.6. Statistical Analysis. Statistical analysis was performed using Prism (v8, GraphPad Software, San Diego, CA) to determine differences in offspring outcomes based on the exposure group. One-way analysis of variance (ANOVA) with Tukey's multiple comparisons tests or non-parametric equivalent were conducted. An adjusted p value of <0.05 was considered statistically significant.

3. RESULTS AND DISCUSSION

3.1. UFP Characterization. Particle size range was $0.02\text{--}0.5 \mu\text{m}$ as indicated in Figure 1A,B for both LD and HD chambers. The peak particle diameter was 0.034 and $0.052 \mu\text{m}$ (34 and 52 nm) for LD and HD, respectively, over the entire exposure period within the UFP range. The mean PM mass concentration for the LD and HD exposures over the time course of each exposed pregnant dam averaged 54.59 ± 4.62 and $272.96 \pm 8.64 \mu\text{g}/\text{m}^3$ (SD), respectively, as determined by the real-time mass concentration system (Figure S2). Our initial murine model created by Rychlik et al. 2019 established a daily UFP exposure at $100 \mu\text{g}/\text{m}^3$ throughout gestation, equivalent to $25 \mu\text{g} \text{ m}^{-3}/24 \text{ h}$, slightly under the U.S. EPA 24 h standard $35 \mu\text{g} \text{ m}^{-3}$. In that model, offspring challenged with house dust mite from 1 to 4 weeks of age demonstrated an immunosuppressive phenotype more pronounced in the C57Bl/6 strain than the BALB/c strain. We adapted that model to our current study utilizing C57Bl/6n mice, generating levels at ~ 55 and $\sim 275 \mu\text{g}/\text{m}^3$ for 6 h daily throughout gestation, equivalent to ~ 13.75 and $\sim 68.75 \mu\text{g}$

$\text{m}^{-3}/24 \text{ h}$, herein referred to as the LD and HD groups, respectively. Previously, Behlen et al. 2021 showed sex- and dose-specific changes in offspring birth outcomes, placental morphology, and transcriptomic changes, with the most pronounced effects in placenta from female offspring exposed to a similar LD level. This is the first study to our knowledge to investigate dose- and sex-specific outcomes in offspring respiratory infection following prenatal UFP exposure.

3.2. Reduced Neonate Body Weight in Response to RSV Infection following LD Maternal UFP Exposure. The average maternal weight gain did not vary significantly across exposure groups (Figure S3). We have consistently observed no impact on maternal weight gain in our other experiments employing similar LD and HD exposures.^{12,19} Initial offspring body weights measured on postnatal day (PND) 5 showed no significant differences among mean pup weights across exposure groups (Figure S4). This was somewhat surprising because human observational studies support an impact of PM on infant birth weight.²⁰ Some exposure models do reflect effects on birth weight; however, Rychlik et al. 2019 also did not observe offspring weight changes in response to prenatal UFPs. Behlen et al. 2021 noted reduced female fetal crown to rump lengths in the LD exposed group. Weights evaluated at the time point in the current model (PND5) may not manifest at this stage. Moreover, effects may not be uncovered until a subsequent challenge. For instance, in previous work, effects on offspring body weight were only observed in offspring with combined paternal and maternal environmental exposures (Table 1).²¹

Offspring body weight was also measured after viral or sham challenge at either 3 or 9 dpi, corresponding to PND 8 or 14, respectively. No significant differences were detected 3 dpi between exposure groups, even when sex was taken into consideration (data not shown). Notably, 9 dpi, mean pup body weight in the LD RSV group ($6.15 \pm 0.16 \text{ g}$) was significantly lower than the HD RSV group ($6.86 \pm 0.20 \text{ g}$) (Figure 2). This was reflected in the female offspring, which showed a significant decrease ($\sim 12.9\%$) in the LD RSV mean weight in comparison to the experimental control (FA Sham, $7.06 \pm 0.36 \text{ g}$). In their model of neonatal PM exposure and influenza infection, Lee et al. also noted PM-exposed pups gained significantly less weight in comparison to control groups, highlighting enhanced morbidity.¹⁰ Interestingly in our model, we did not observe a linear dose-response relationship

Table 1. Pulmonary Inflammation Following *In Utero* Exposure to UFPs and Offspring RSV Challenge^a

	overall	males	females
FA Sham	0.27 ± 0.14	0.14 ± 0.14	0.50 ± 0.29
LD Sham	0.44 ± 0.24	0.60 ± 0.40	0.25 ± 0.25
HD Sham	0.22 ± 0.15	0.20 ± 0.20	0.25 ± 0.25
FA RSV	0.43 ± 0.30	0.67 ± 0.67	0.25 ± 0.25
LD RSV	0.60 ± 0.22	0.57 ± 0.30	0.67 ± 0.33
HD RSV	0.73 ± 0.30	1.17 ± 0.48	0.20 ± 0.20

^aHistological evaluation was performed on H&E stained slides using a scoring system ranging from 0 to 3 (0-no lesions; 1-mild; 2-moderate; 3-marked). Average scores, shown above ± SEM, were compared among groups and sexes. Offspring sample sizes for histopathology include FA Sham ($n = 7, 4, 3$), LD Sham ($n = 5, 4, 4$), HD Sham ($n = 5, 4, 4$), FA RSV ($n = 3, 4, 3$), LD RSV ($n = 7, 3, 4$), and HD RSV ($n = 6, 5, 6$). Data is represented as mean ± SEM.

in decreased body weight. In fact, the HD-exposed, RSV-infected pups weighed significantly more than the LD RSV group in combined sex data. This may be influenced by differences in initial litter sizes. The average litter size of the LD-exposed dams (9.1 ± 2.2 pups) was significantly higher than HD-exposed dams (6.7 ± 0.8 pups). Still, sex-specificity indicating female susceptibility could be an underlying factor since phenotypic differences were also pronounced in data published by Behlen et al. using similar exposures (FA, LD, and HD). Findings show distinct changes in the female LD-exposed offspring that was not as marked in the HD group. This “U-shaped curve” or potential “thresholding effect” is also observed for some, but not all, of the additional female phenotypes described below.

3.3. Increased Expression of Oxidative Stress and Inflammation-Related Genes in Male Offspring Lung following HD Maternal UFP Exposure. We performed qRT-PCR in lung samples collected 9 dpi to evaluate expression of three genes (*Nrf2*, *Nqo1*, and *NF-κB*) (Figure 3). Expression was significantly increased in all three genes in male offspring prenatally exposed to HD (~4-fold) compared to control. Females had notably lower gene expression that did not vary significantly between groups. NRF2 is a redox sensitive transcription factor regarded as the master regulator of the antioxidant response, also important in immune responses.²² NRF2 binding to an antioxidant response element

(ARE) in promoters upstream of phase II enzymes and other oxidative stress-related enzymes, including NQO1, drives transcription in response to oxidative stress. Disruption of the *Nrf2* gene has been shown to enhance susceptibility to allergic airway inflammatory responses induced by chronic exposure to diesel exhaust PM²³ and increase disease severity in an adult model of RSV infection.²⁴ In our model, NRF2 is activated in response to HD exposure in male offspring lung, evidenced by increased expression of *Nrf2* and downstream gene *Nqo1* in sham- and RSV-infected male offspring exposed prenatally to HD. *NF-κB* is also increased in both of these groups (sham and RSV) in male offspring exposed to HD. *NF-κB* is a redox-sensitive transcription factor that activates pro-inflammatory cytokines and other immune response genes. Activation of this pathway is associated with increased levels of the pro-inflammatory enzyme COX-2 and cytokines like IL-1β and TNF-α. Changes in these genes may underlie differential outcomes in male and female offspring.

3.4. Pulmonary Inflammation in Response to RSV Varies in Male and Female Offspring by Maternal UFP Dose. Allowing for time for a sufficient immune response, offspring BALF was collected 9 dpi and evaluated for a total leukocyte count and a leukocyte differential. The total number of leukocytes within all sham groups were similar, all close to 100 leukocytes/μL. Overall, BALF from the LD RSV group demonstrated the highest leukocyte/μL total (118.4 ± 9.1) (Figure S6). However, no significant differences were observed among any of the sex-separated groups. Leukocyte differentials demonstrated a predominance of mononuclear cells, typical of BALF samples, with smaller and variable numbers of lymphocytes, neutrophils, and eosinophils (data not shown). No statistical significances were observed across groups within the mononuclear cells, lymphocytes, or neutrophils.

Additionally, offspring lungs were fixed at 9 dpi in a subset of offspring and stained with H&E to evaluate severity of inflammation. Histological scores (Table 1) indicate maternal UFP exposure enhanced lung pathology distinctly across sex. Representative images are shown in Figure 4. Peribronchiolar and perivascular infiltrates of eosinophils and macrophages were the most common inflammatory finding, with eosinophilic alveolar infiltrates and hyperplasia of the bronchiole-associated lymphoid tissue being less common. Mild alveolar histiocytosis was seen in nearly every specimen ($n = 54$), with

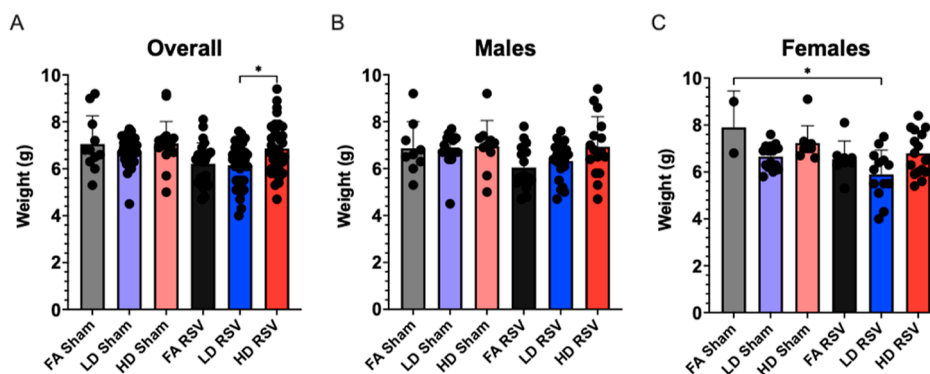


Figure 2. Offspring weights measured 9 days post-infection expressed as mean ± SEM. (A) Overall, offspring body weights were significantly lower in the LD RSV group, as compared with the HD RSV group ($p = 0.0324$). (B) Differences between body weights post-infection did not vary significantly in male offspring. (C) In females, offspring from the LD RSV group weighed significantly less than the FA Sham group ($p = 0.0132$). Offspring sample sizes from 2 to 6 litters, listed ($n =$ male, female), include FA Sham (9, 2), LD Sham (16, 15), HD Sham (10, 9), FA RSV (16, 8), LD RSV (20, 13), and HD RSV (16, 16). Data analyzed using one-way ANOVA with Tukey's multiple comparison test (* $P < 0.05$).

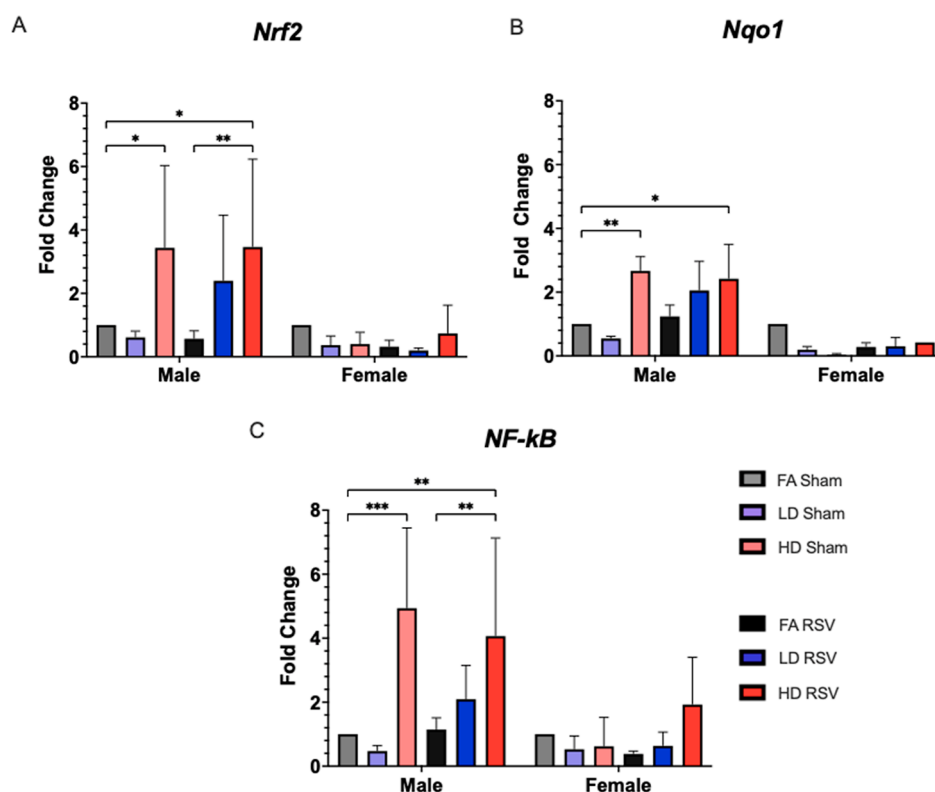


Figure 3. Genes related to oxidative stress and inflammatory response were evaluated in lung tissue collected 9 days post-infection. Males from the HD Sham and HD RSV groups showed significant increases in expression, up to 4 fold, from their controls for *Nrf2* (A), *Nqo1* (B), *NF-κB* (C), while no female groups displayed significantly different levels of expression. Offspring sample sizes from 3 to 6 litters, listed as ($n = \text{male, female}$) include FA Sham (6, 1), LD Sham (4, 3), HD Sham (7, 8), FA RSV (8, 7), LD RSV (5, 4), and HD RSV (7, 4). Error bars represent SEM. Data analyzed using one-way ANOVA with Tukey's multiple comparison test (* $p < 0.05$; ** $p < 0.01$; *** $p < 0.001$).

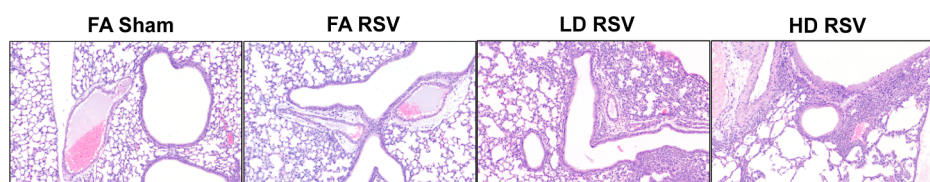


Figure 4. Scoring system was applied to evaluate severity of pulmonary inflammation. Representative photomicrographs of H&E-stained sections of lungs collected 9 days post-infection showing no inflammation (grade 0) in the FA Sham group, mild inflammation (grade 1) in the FA RSV group, moderate inflammation (grade 2) in the LD RSV group, and marked inflammation (grade 3) in the HD RSV group. Scale = 100 μm . Average scores by offspring sex shown in Table 1.

moderate alveolar histiocytosis ($n = 4$) being associated with moderate to marked levels of inflammation in 3 of 4 samples. In the sham-exposed groups, almost all mice were classified with either mild inflammation (FA 27.0%, LD 22.2%, and HD 22.2%) or no inflammation (FA 73.0%, LD 66.6%, and HD 77.8%), except for one mouse in the LD Sham group that scored moderate (11.1%). Generally, males in the HD-RSV group had the most marked inflammation (overall score, 1.17 ± 0.48), whereas females in the LD-RSV group showed more cases of mild and some marked inflammation (overall score, 0.67 ± 0.33). Lung sections were also stained with the PAS stain to examine the goblet cells and mucus production of the bronchi and bronchioles. The PAS stain did occasionally highlight aggregates of mucus within the lumen of airways ($n = 2$) but did not reveal any significant association between severity of inflammation and mucus production nor were there statistical differences between exposure groups (Table S1).

We also evaluated the presence of replicating RSV using the TCID₅₀ assay in offspring lungs collected 3 dpi (Figure S5), a time point selected due to peak levels based on viral load kinetics.²⁵ As expected, none of the sham-exposed pups across any maternal exposure group showed evidence of any CPE that would signify viral replication. Overall, lungs from RSV-infected pups generally demonstrated increasing numbers of virions/mL in correlation with exposure: FA-RSV (6576 ± 5020), LD-RSV ($14,326 \pm 6240$), and HD-RSV ($33,035 \pm 14,665$ virions/mL). One outlier ($56,2341$ virions/mL) within the LD-RSV group had an exponential difference from the mean of the group and was removed.

Our model demonstrated the successful infection of neonates with a chimeric strain of RSV, with histologic evidence of an inflammatory response predominated with eosinophils and mononuclear cells. RSV is historically problematic in inducing infection mice; however, the rA2-19F strain has been shown to replicate key immunological

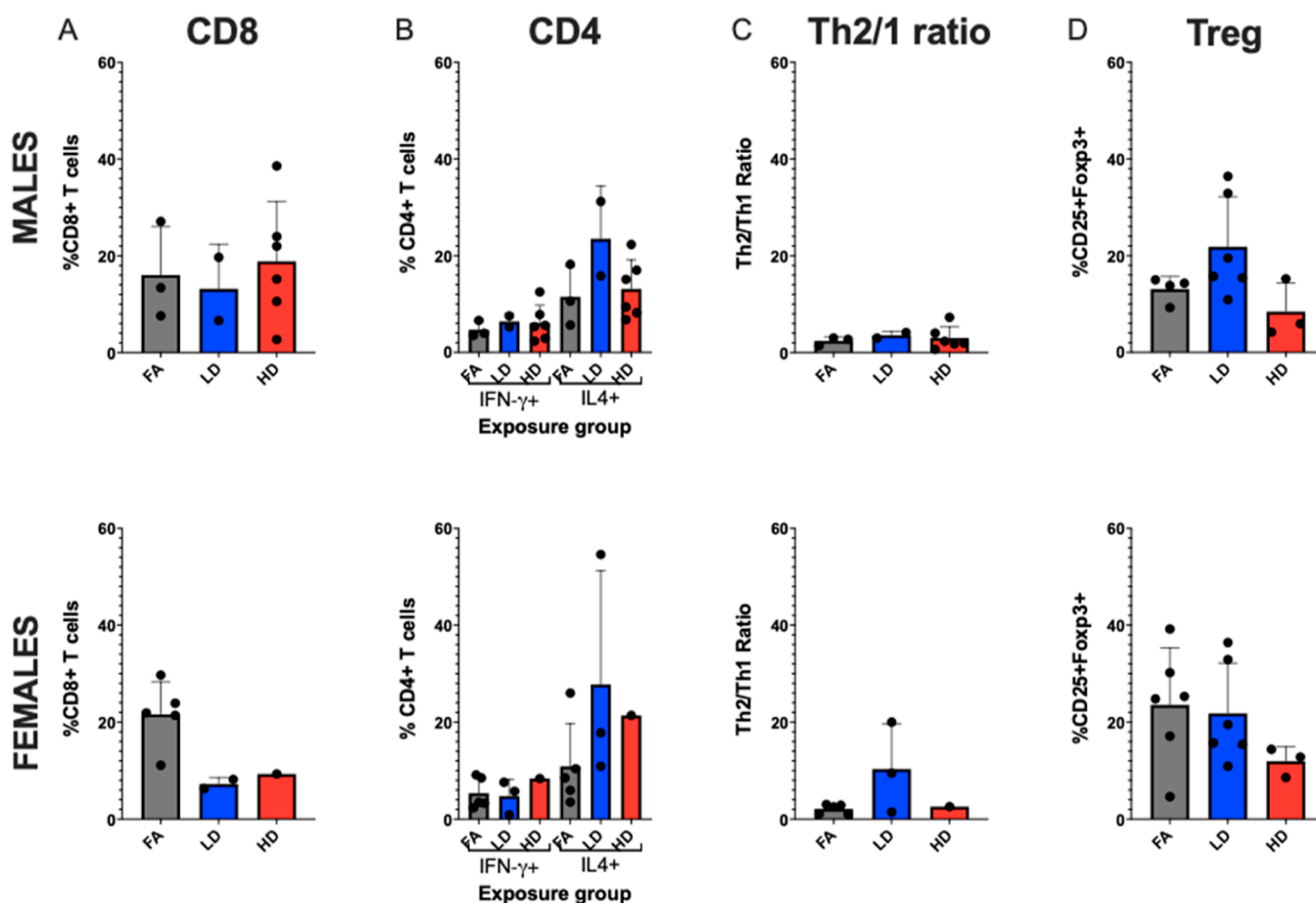


Figure 5. Flow cytometry analysis of offspring lungs 9 days post-infection, separated by sex. (A) CD8+ T cells. (B) CD4+ T cells differentiated by Th1 (IFN- γ + cells) and Th2 (IL-4+ cells). (C) Th1/Th2 ratios. (D) T regulatory (Treg) cells (CD25+Foxp3+). Offspring sample sizes from 3 to 6 litters, listed as (n = male, female) for A–C and D, respectively, include FA RSV (3, 5) and (4, 6), LD RSV (2, 2) and (6, 6), and HD RSV (6, 1) and (3, 3). Error bars represent SEM. Data analyzed using one-way ANOVA with Tukey’s multiple comparison test.

features of human infant infection in neonatal mouse models.^{25,26} The TCID₅₀ assay demonstrated CPE within cells cultured with infected lung homogenates, indicating pathogenicity of the virus within our *in vivo* model. Notably, histological scores indicating the greatest amount of inflammation were observed in the male HD group, and female LD group, suggesting differential dose effects by sex. Overall, these findings support prenatal UFP exposure enhances neonatal RSV infection severity. Outcomes from our model corroborate findings from human observational studies.^{7,8} Importantly, our LD maternal exposure, under the U.S. EPA 24 h exposure level for PM_{2.5} also implied increased offspring risk, as did findings from Jedrychowski et al.⁸ showing risk for acute bronchitis and pneumonia in children prenatally exposed to levels below 35 $\mu\text{g}/\text{m}^3$. Moreover, our findings also agree with associations observed by Darrow et al. citing increased risk of hospitalization for pneumonia and associations with bronchiolitis/bronchitis among children aged 1–4 years exposed to various PM fractions, including organic carbon and sulfates, both represented in our exposure model. A recent study published by Fang et al. showed increased childhood respiratory emergency room visits among children under 14 living in Beijing in association with exposures to particles in size fractions of 5–560 nm, mainly from traffic emissions.⁹ Significant associations of respiratory emergency room visits were also found to be associated with secondary aerosols and

emissions from gasoline and diesel vehicles. The findings by Fang et al. corroborate our model findings specific to UFP-exacerbated childhood respiratory risks.

Early life UFP exposure may exert a detrimental influence over the neonate’s ability to combat RSV infection. Mucous metaplasia and hypersecretion are commonly seen in children with RSV and is one of the main components of airway obstruction;^{13,14} these findings are mirrored in animal models.²⁷ However, in our model, when comparing the goblet cell counts, no relationships were observed within the UFP-exposed groups, though a few individual mice were noted to have accumulations of mucin within bronchi. This lack of goblet cell metaplasia is most likely due to the short duration of infection in mice, even with chimeric strain of the virus and maybe more pronounced in a re-infection study.

3.5. In Utero UFP Exposure and Offspring T Cell Response to RSV Infection. Offspring lungs challenged with RSV were also collected 9 dpi to evaluate T cell differentiation (Figure 5). There were no significant differences among the CD8+ T cell population among exposure groups, although a slight decrease in the LD group (12.54 ± 3.40) was observed as compared to the FA (19.51 ± 2.80) and HD (17.49 ± 4.49) groups, indicating possible decreased Th1 response. This coincided with a tendency toward Th2 bias (i.e., increased CD4+IL4+ T cells), especially in the LD group. CD4+IFN- γ + cell levels were consistently low across the FA, LD, and HD

groups, and the percentage of CD4+ cells staining for IL-4 was higher in all groups, with LD-RSV group average (26.06 ± 7.88), higher than both the FA and the HD groups by 15 and 11%, respectively. Within the Treg panel, offspring average CD25+Foxp3+ cells did not differ significantly across groups overall. Sex-separated data show similar patterns. Overall, the flow cytometry data mirror our histopathological findings indicating again a potential non-monotonic dose–response or “thresholding” effect. An altered Th1/Th2 ratio, skewed toward Th2 response reflects the typical pattern of immune response in children who have increased RSV severity due to an enhanced Th2/allergic immunophenotype.²⁸ Human observational support PM_{2.5} affects the immune system, although only a handful of human studies relevant to early-life exposure are published to date.^{29,30} Herr et al. observed that prenatal exposure to PM_{2.5} shifted lymphocyte distributions in umbilical cord blood, where exposure during early gestation resulted in increased T lymphocytes, decreased B lymphocytes, and natural killer cells, and late gestation exposure was associated with decreased T lymphocytes, increased B lymphocytes, and natural killer cells.³¹ Evidence of shifting immune responses over different developmental stages is also reflected in mouse models. Wang et al. showed gestational exposure to combustion-derived PM_{0.1} inhibited offspring pulmonary T cell development, with suppression of Th1, Th2, Th17, and Tregs at six days of age.³² Pulmonary Th1 cells remained suppressed up to six weeks, leading to enhancement of postnatal allergic responses to OVA evidenced by increased airway eosinophilia driven by Th2-bias responses. In another model, Sharkhuu et al. (2010) demonstrated prenatal diesel exhaust (DE) exposure caused sex-specific alterations in lung protein and inflammatory cells, as well as splenic T cell subsets, even though allergen challenge did not enhance inflammation. These findings mirror data in our previous UFP (LD, 100 $\mu\text{g}/\text{m}^3$), allergen (HDM) model, wherein Rychlik et al. also did not observe prenatal UFP to enhance inflammatory response to allergen. Overall, this window of immune suppression may in fact underlie increased susceptibility to viral infection. Findings from the current research add to the body of basic research showing prenatal PM_{0.1} exposure alters offspring pulmonary immune system development, signifying risk for acute respiratory infection risk.

Overall, our findings demonstrate *in utero* UFP exposure alters offspring pulmonary immune responses in a sex- and dose-specific manner. Since RSV infection is a significant cause of infant morbidity and mortality, policies and interventions to reduce early life air pollution exposure and impact on acute respiratory disease are likely to have a large public health impact and are therefore highly warranted. Our model has some limitations. First, a few of our measures with small sample sizes prevented robust sex-separated statistics. Another limitation is our selection of the background strain, the C57Bl/6, which is known for having a Th1-biased immune system. C57Bl/6 mice are considered moderate responders to RSV according to the ranking done by High et al.³³ We chose this strain since in our previous work Rychlik et al. showed higher strain susceptibility to prenatal UFP exposure. However, the inherent Th1-biased immunophenotype may have masked differential results in some endpoints. Future research on strain effects is warranted. Last, the viral titer employed was also somewhat low in comparison to other reports,²⁵ which also likely could have masked more significant effects. Evenson, our model has several strengths, including a highly controllable

maternal inhalation throughout gestation representing urban UFP exposure. This model lays the foundation for future mechanistic investigations to characterize sex differences in respiratory responses to prenatal UFP exposure.

■ ASSOCIATED CONTENT

Supporting Information

The Supporting Information is available free of charge at <https://pubs.acs.org/doi/10.1021/acs.est.2c02786>.

Additional methodological details and results, including UFP exposure averages, maternal and neonatal weights, pulmonary viral load, BALF data, histopathology scores, and flow cytometry gating strategies (PDF)

■ AUTHOR INFORMATION

Corresponding Author

Natalie M. Johnson – Department of Environmental and Occupational Health, Texas A&M University, College Station, Texas 77843, United States; orcid.org/0000-0001-8584-9713; Phone: 979-436-9325; Email: nmjohnson@tamu.edu

Authors

Carmen Lau – Department of Veterinary Pathobiology, Texas A&M University, College Station, Texas 77843, United States

Jonathan C. Behlen – Department of Environmental and Occupational Health, Texas A&M University, College Station, Texas 77843, United States

Alexandra Myers – Department of Veterinary Pathobiology, Texas A&M University, College Station, Texas 77843, United States

Yixin Li – Department of Chemistry, Texas A&M University, College Station, Texas 77843, United States

Jiayun Zhao – Department of Chemistry, Texas A&M University, College Station, Texas 77843, United States

Navada Harvey – Department of Environmental and Occupational Health, Texas A&M University, College Station, Texas 77843, United States

Gus Wright – Department of Veterinary Pathobiology, Texas A&M University, College Station, Texas 77843, United States

Aline Rodrigues Hoffmann – Department of Comparative, Diagnostic & Population Medicine, University of Florida, Gainesville, Florida 32611, United States

Renyi Zhang – Department of Chemistry and Department of Atmospheric Sciences, Texas A&M University, College Station, Texas 77843, United States; orcid.org/0000-0001-8708-3862

Complete contact information is available at:

<https://pubs.acs.org/10.1021/acs.est.2c02786>

Author Contributions

The manuscript was written through contributions of all authors. Credits: conceptualization (C.L., N.M.J., and A.R.H.), methodology (N.H., G.W., J.B., and Y.L.), formal analysis (C.L., A.M., J.Z., and A.R.H.), investigation (C.L., J.B., and A.M.), resources (R.Z.), writing—original draft (C.L.), writing—review and editing (N.M.J., A.R.H., and R.Z.), supervision (N.M.J., A.R.H., and R.Z.), and funding acquisition (N.M.J.). All authors have given approval to the final version of the manuscript.

Funding

This study was supported by the National Institute of Environmental Health Sciences grant R01ES02886. C.L. was funded by T32OD011083. R.Z. also received funding from Robert A. Welch Foundation A-1419.

Notes

The authors declare no competing financial interest.

ACKNOWLEDGMENTS

The authors would like to thank the members of Texas Institute for Genomic Medicine (TIGM), particularly Drs. Ben Morpurgo and Andrei Golovko. Additional thanks are extended to Dr. Ivan Rusyn for providing the exposure chambers and Dr. Martin Moore for providing the chimeric RSV strain. The authors recognize the NIEHS Outstanding New Environmental Scientist (ONES) external advisory board members Drs. Stephania Cormier, Steve Kleeberger, and Dave Williams for their feedback on building this model. Last, we appreciate support from Dr. Natalie Johnson's laboratory personnel including Drew Pendleton, Ross Shore, Toriq Mustapha, Dennis Garcia-Rhodes, Amandeep Brar, and Tiffanie Vargas.

ABBREVIATIONS

UFP ultrafine particulate matter
GD gestational day
PND postnatal day
dpi days post-infection

REFERENCES

- (1) Glinianaia, T. D. H.; Rankin, V.; Bell, J.; Pless-Mulloli, R.; Howel, D. Does Particulate Air Pollution Contribute to Infant Death? A Systematic Review. *Environ. Health Perspect.* **2004**, *112*, 1365–1370.
- (2) DeFranco, E.; Hall, E.; Hossain, M.; Chen, A.; Haynes, E. N.; Jones, D.; Ren, S.; Lu, L.; Muglia, L. Air pollution and stillbirth risk: Exposure to airborne particulate matter during pregnancy is associated with fetal death. *PLoS One* **2015**, *10*, No. e0120594.
- (3) Percy, Z.; DeFranco, E.; Xu, F.; Hall, E. S.; Haynes, E. N.; Jones, L. J.; Muglia, A.; Chen, A. Trimester Specific PM 2.5 Exposure and Fetal Growth in Ohio, HHS Public Access. *Environ. Res.* **2019**, *171*, 111–118.
- (4) Health Effects Institute. *State of Global Air 2019*; Health Effects Institute, 2019; p 24.
- (5) Johnson, N. M.; Rodrigues-Hoffmann, A.; Behlen, J. C.; Lau, C.; Pendleton, D.; Harvey, N.; Shore, R.; Li, Y.; Chen, J.; Tian, Y.; Zhang, R. Air pollution and children's health—a review of adverse effects associated with prenatal exposure from fine to ultrafine particulate matter. *Environ. Health Prev. Med.* **2021**, *26*, 72.
- (6) Korten, I.; Ramsey, K.; Latzin, P. Air pollution during pregnancy and lung development in the child. *Paediatr. Respir. Rev.* **2017**, *21*, 38–46.
- (7) Darrow, L. A.; Klein, M.; Flanders, W. D.; Mulholland, J. A.; Tolbert, P. E.; Strickland, M. J. Air pollution and acute respiratory infections among children 0-4 years of age: An 18-year time-series study. *Am. J. Epidemiol.* **2014**, *180*, 968–977.
- (8) Jedrychowski, W. A.; Perera, F. P.; Spengler, J. D.; Mroz, E.; Stigter, L.; Flak, E.; Majewska, R.; Klimaszewska-Rembiasz, M.; Jacek, R. Intrauterine exposure to fine particulate matter as a risk factor for increased susceptibility to acute broncho-pulmonary infections in early childhood. *Int. J. Hyg. Environ. Health* **2013**, *216*, 395–401.
- (9) Fang, J.; Song, X.; Xu, H.; Wu, R.; Song, J.; Xie, Y.; Xu, X.; Zeng, Y.; Wang, T.; Zhu, Y.; Yuan, N.; Jia, J.; Xu, B.; Huang, W. Associations of ultrafine and fine particles with childhood emergency

room visits for respiratory diseases in a megacity. *Thorax* **2021**, *77*, 391.

(10) Lee, G. I.; Saravia, J.; You, D.; Shrestha, B.; Jaligama, S.; Hebert, V. Y.; Dugas, T. R.; Cormier, S. A. Exposure to combustion generated environmentally persistent free radicals enhances severity of influenza virus infection. *Part. Fibre Toxicol.* **2014**, *11*, 57.

(11) Jalgama, S.; Saravia, J.; You, D.; Yadav, N.; Lee, G. I.; Shrestha, B.; Cormier, S. A. Regulatory T cells and IL10 suppress pulmonary host defense during early-life exposure to radical containing combustion derived ultrafine particulate matter. *Respir. Res.* **2017**, *18*, 15.

(12) Rychlik, K. A.; Secrest, J. R.; Lau, C.; Pulczynski, J.; Zamora, M. L.; Leal, J.; Langlely, R.; Myatt, L. G.; Raju, M.; Chang, R. C. A.; Li, Y.; Golding, M. C.; Rodrigues-Hoffmann, A.; Molina, M. J.; Zhang, R.; Johnson, N. M. In utero ultrafine particulate matter exposure causes offspring pulmonary immunosuppression. *Proc. Natl. Acad. Sci. U.S.A.* **2019**, *116*, 3443–3448.

(13) Bohmwald, K.; Espinoza, J. A.; Rey-Jurado, E.; Gómez, R. S.; González, P. A.; Bueno, S. M.; Riedel, C. A.; Kalergis, A. M. Human Respiratory Syncytial Virus: Infection and Pathology. *Semin. Respir. Crit. Care Med.* **2016**, *37*, 522.

(14) Borchers, A. T.; Chang, C.; Gershwin, M. E.; Gershwin, L. J. Respiratory syncytial virus - A comprehensive review. *Clin. Rev. Allergy Immunol.* **2013**, *45*, 331–379.

(15) Collins, P. L.; Graham, B. S. Viral and Host Factors in Human Respiratory Syncytial Virus Pathogenesis. *J. Virol.* **2008**, *82*, 2040.

(16) Hall, P.; Weinberg, C.; Iwane, G. A.; Blumkin, M. K.; Edwards, A. K.; Staat, K. M.; Auinger, M. A.; Griffin, P.; Poehling, K. A.; Erdman, R.; Grijalva, K. A.; Zhu, D.; Szilagyi, C. G.; Zhu, Y. The Burden of Respiratory Syncytial Virus Infection in Young Children Caroline. *N. Engl. J. Med.* **2009**, *360*, 588–598.

(17) Byrne, A. J.; Weiss, M.; Mathie, S. A.; Walker, S. A.; Eames, H. L.; Saliba, D.; Lloyd, C. M.; Udalova, I. A. A critical role for IRF5 in regulating allergic airway inflammation. *Mucosal Immunol.* **2017**, *10*, 716–726.

(18) Ramakrishnan, M. A. Determination of 50% endpoint titer using a simple formula. *World J. Virol.* **2016**, *5*, 85.

(19) Behlen, N. M.; Lau, C.; Li, C. H.; Dhagat, Y.; Stanley, P.; Rodrigues Hoffman, J. A.; Golding, R.; Zhang, R.; Johnson, M. C.; Zhang, R. Gestational exposure to ultrafine particles reveals sex- and dose-specific changes in offspring birth outcomes, placental morphology, and gene networks. *Toxicol. Sci.* **2021**, *184*, 204–213.

(20) Uwak, I.; Olson, N. ; Fuentes, A.; Moriarty, M.; Pulczynski, J.; Lam, J.; Xu, X.; Taylor, B. D.; Taiwo, S.; Koehler, K.; Foster, M.; Chiu, W. A.; Johnson, N. M. Application of the navigation guide systematic review methodology to evaluate prenatal exposure to particulate matter air pollution and infant birth weight. *Environ. Int.* **2021**, *148*, 106378.

(21) Mustapha, T. A.; Chang, R. C.; Garcia-Rhodes, D.; Pendleton, D.; Johnson, N. M.; Golding, M. C. Gestational exposure to particulate air pollution exacerbates the growth phenotypes induced by preconception paternal alcohol use: a multiplex model of exposure. *Environ. Epigenet.* **2020**, *6*, 1–6.

(22) Silva-Islas, C. A.; Maldonado, P. D. Canonical and non-canonical mechanisms of Nrf2 activation. *Pharmacol. Res.* **2018**, *134*, 92–99.

(23) Li, N.; Alam, N.; Venkatesan, J.; Eiguren-Fernandez, M. I.; Schmitz, A.; Di Stefano, D.; Slaughter, E.; Killeen, N.; Wang, E.; Huang, X.; Wang, A.; Miguel, M.; Cho, A. H.; Sioutas, A.; Nel, C.; Nel, A. E. Nrf2 Is a Key Transcription Factor That Regulates Antioxidant Defense in Macrophages and Epithelial Cells: Protecting against the Proinflammatory and Oxidizing Effects of Diesel Exhaust Chemicals. *J. Immunol.* **2004**, *173*, 3467–3481.

(24) Cho, H. Y.; Imani, H. Y.; Miller-DeGraff, F.; Walters, L.; Melendi, D.; Yamamoto, G. A.; Polack, M.; Kleeberger, F. P.; Kleeberger, S. R. Antiviral activity of Nrf2 in a murine model of respiratory syncytial virus disease. *Am. J. Respir. Crit. Care Med.* **2009**, *179*, 138–150.

(25) You, D.; Siefker, D. T.; Shrestha, B.; Saravia, J.; Cormier, S. A. Building a better neonatal mouse model to understand infant respiratory syncytial virus disease. *Respir. Res.* **2015**, *16*, 91.

(26) Cormier, S. A.; You, D.; Honnegowda, S. The Use of a Neonatal Mouse Model to Study Respiratory Syncytial Virus Infections. *Expert Rev. Anti Infect. Ther.* **2010**, *8*, 1371.

(27) Gitiban, N.; Jurcisek, J. A.; Harris, R. H.; Mertz, S. E.; Durbin, R. K.; Bakaletz, L. O.; Durbin, J. E. Chinchilla and Murine Models of Upper Respiratory Tract Infections with Respiratory Syncytial Virus. *J. Virol.* **2005**, *79*, 6035–6042.

(28) Becker, Y. Respiratory syncytial virus (RSV) evades the human adaptive immune system by skewing the Th1/Th2 cytokine balance toward increased levels of Th2 cytokines and IgE, markers of allergy—a review. *Virus Genes* **2006**, *33*, 235–252.

(29) Wu, J.; Zhong, T.; Zhu, Y.; Ge, D.; Lin, X.; Li, Q. Effects of particulate matter (PM) on childhood asthma exacerbation and control in Xiamen, China. *BMC Pediatr.* **2019**, *19*, 194.

(30) Morales-Rubio, R. A.; Alvarado-Cruz, I.; Manzano-León, N.; Andrade-Oliva, M.; Uribe-Ramirez, M.; Quintanilla-Vega, B.; Osornio-Vargas, A.; De Vizcaya-Ruiz, A. In utero exposure to ultrafine particles promotes placental stress-induced programming of renin-angiotensin system-related elements in the offspring results in altered blood pressure in adult mice. *Part. Fibre Toxicol.* **2019**, *16*, 7.

(31) Herr, C. E. W.; Dostal, E. W.; Ghosh, M.; Ashwood, R.; Lipsett, P.; Pinkerton, M.; Sram, K. E.; Hertz-Picciotto, R. Air pollution exposure during critical time periods in gestation and alterations in cord blood lymphocyte distribution: a cohort of livebirths. *Environ. Health* **2010**, *9*, 46.

(32) Wang, P.; You, D.; Saravia, J.; Shen, H.; Cormier, S. A. Maternal exposure to combustion generated PM inhibits pulmonary Th1 maturation and concomitantly enhances postnatal asthma development in offspring. *Part. Fibre Toxicol.* **2013**, *10*, 29.

(33) High, M.; Cho, H.-Y.; Marzec, J.; Wiltshire, T.; Verhein, K. C.; Caballero, M. T.; Acosta, P. L.; Cienciewicki, J.; McCaw, Z. R.; Kobzik, L.; Miller-DeGraff, L.; Gladwell, W.; Peden, D. B.; Serra, M. E.; Shi, M.; Weinberg, C.; Suzuki, O.; Wang, X.; Bell, D. A.; Polack, F. P.; Kleeberger, S. R. Determinants of host susceptibility to murine respiratory syncytial virus (RSV) disease identify a role for the innate immunity scavenger receptor MARCO gene in human infants. *EBioMedicine* **2016**, *11*, 73–84.